The 8th European Congress on Computational Methods in Applied Sciences and Engineering

ECCOMAS Congress 2022

5 – 9 June 2022, Oslo, Norway

Lessons Learnt from Chimera Method Application to a Deploying Krueger Device

APURVA HASABNIS1, HANS MASELAND2, FRÉDÉRIC MOENS3, ALEŠ PRACHAŘ4 & JOCHEN WILD1

[1] German Aerospace Center (DLR)
Lilienthalplatz 7,38108 Braunschweig, Germany
email: apurva.hasabnis@dlr.de

[2] Royal Netherlands Aerospace Centre (NLR)
Amsterdam, The Netherlands
email: hans.maseland@nlr.nl

[3] French Aerospace Lab (ONERA)
Meudon, France
email: frederic.moens@onera.fr

[4] Czech Aerospace Research Centre (VZLU)
Prague, Czech Republic
email: prachar@vzlu.cz

Key Words: Aerodynamics, Unsteady, High-Lift Systems, CFD, Chimera, Overset Methods.

1. INTRODUCTION

The Chimera method is an established method for simulation of overlapping grids. Meshing parts independently has made this method popular for complex geometries as well as moving bodies like propellers and rotors or control surfaces. It is thus a promising method to simulate deflecting high-lift systems.

In the frame of the UHURA project, several partners applied their CFD capabilities based on Chimera in order to validate the method for this specific application in comparison to wind tunnel tests. The presentation outlines the different Chimera approaches ranging from structured/2D to hybrid/3D in steady and unsteady simulations for the different type of setups investigated, namely straight and swept wing with full-span and part-span Krueger flap. It summarizes common challenges and best practice for application of the Chimera approach for such a device.

2. KRUEGER PANEL MOTION

The Krueger device movement can be best defined as a multi-body motion, wherein the main wing movement is described w.r.t. the wind-tunnel, the panel w.r.t. the wing and the bullnose w.r.t. the Krueger panel. To implement the Chimera Technique with overlapping meshes, each moving part is Meshed individually and overlapped using various approaches according to individual specifications of the underlying CFD codes. The mesh parameters are chosen depending upon the necessary overlap with the neighbouring moving part.

The components are modelled in a way that there is at least a minor gap between each component. This helps distinguish the components, which is necessary to identify the interpolation points of the overlapping grids to implement the chimera technique.

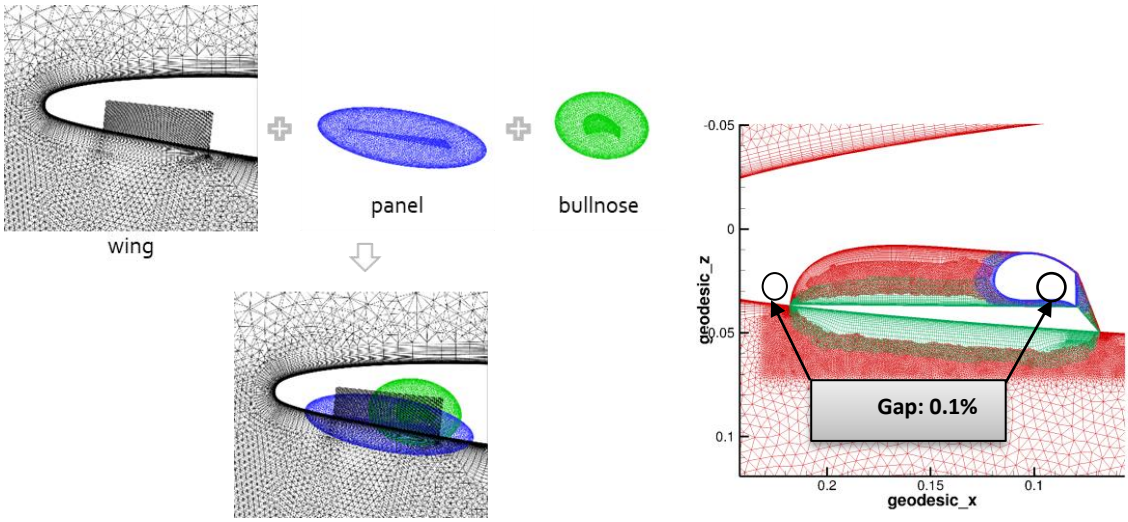

Figure 1: The Chimera technique for Krueger panel set-up

3. DLR-F15-LLE WIND TUNNEL SET-UPS

The wind tunnel tests were carried out at three different wind tunnels at partner locations. Test matrices were set up to try various wind speeds, wing sweeps and panel configurations. The wind velocities were chosen as 30m/s and 45m/s with accelerations ranging from 300, 500 and 1000 m/s2.

3.1 The ONERA wind tunnel

The model at ONERA wind tunnel at Lille, France features a DLR-F15 2D model in wall-to-wall set-up. Part-span and full-span Krueger configurations were tested for static and dynamic deployment on a straight wing. The various tests conducted include wing-pressure distribution, unsteady pressure measurements with MEMS and PIV measurements with up to 20 snapshots deployment giving 7° resolution.

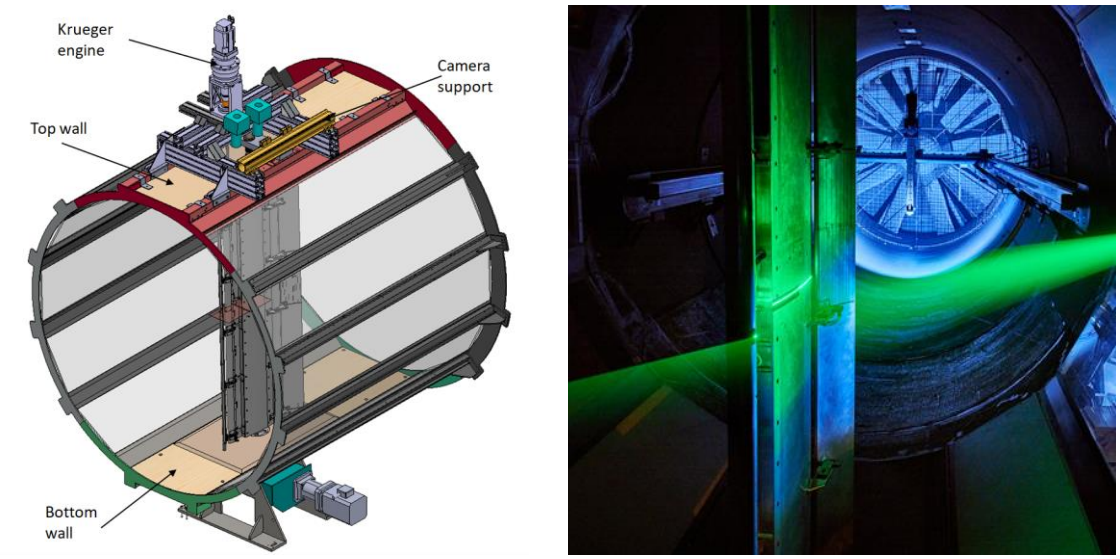

Figure 2: The ONERA wind tunnel set-up

3.2 The DNW-NWB wind tunnel

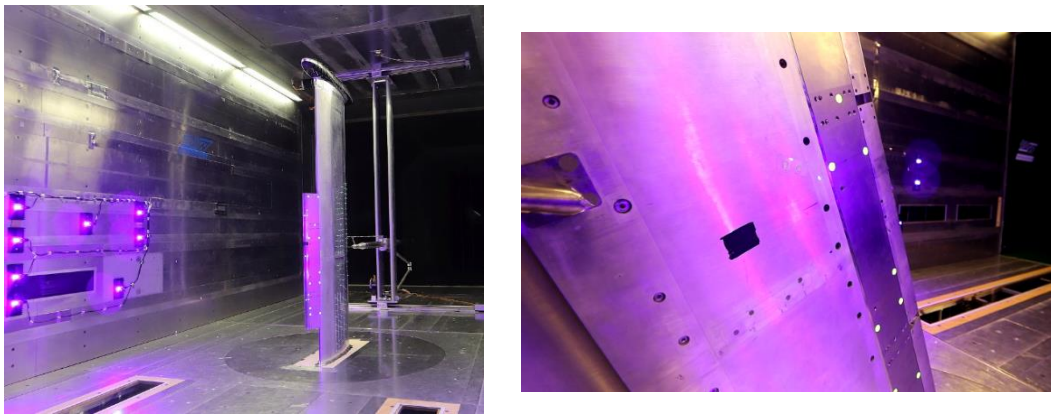

Figure 3: DNW-NWB wind tunnel set-up

The DLR-F15 model was mounted in cantilever configuration in the DNW-NWB tunnel. A part-span Krueger was studied at swept (23°) and unswept wing positions. The test matrix covered static and dynamic deployment of the Krueger device at 30m/s and 45m/s wind speeds. The tests conducted include unsteady pressure measurements using kulites and MEMS, steady pressure measurement using PSI-scanner, study of the wake rake, Krueger deformation (SPR) and Krueger deployment angles.

3.3 The DNW-LLF wind tunnel

Figure 4: DNW-LLF wind tunnel set-up

The larger DLR-F15LS model was mounted in the DNW-LLF low speed, high-Raynold's number facility for analysis. It featured a part-span Krueger at 30 deg sweep in an open test section as shown in the image. The wing pressure distribution was measured along with the unsteady pressure on Krueger with MEMS and PSI. Krueger deformation, deployment angles and PIV flow field were studied.

4. MESHING STRATEGIES

4.1 DLR meshing strategy

The DLR meshing strategy constitutes both, structured and unstructured meshes. Standard prismatic meshes are used around single parts, whereas the global mesh is unstructured. Dependig upon the CFD results obtained, the meshes were further refined to better capture the flow physics. Some of the modifications adopted includes the prismatic mesh around the wing boundary and the wing cavity. It can be seen from the CL graph below that the new mesh v3.3 agrees much better with the experimental results.

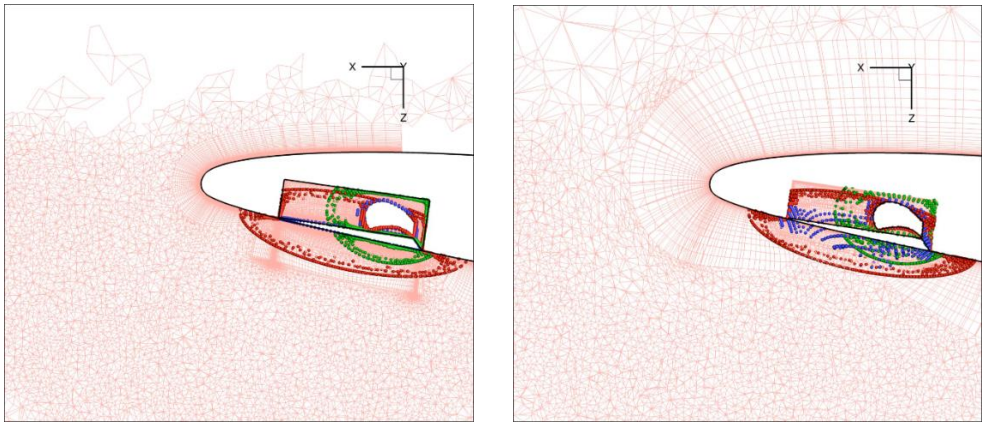

CFD Mesh 2.0 CFD Mesh 3.3 (final)

Figure 5: DLR meshing strategy

There are still certain discrepancies between the experimental and CFD results merely due to lack of available data from experiments. Thus, the data points available for comparison are limited. The pressure coefficients are available only from the pressure integration. It is also understood that a much deeper CFD insight is needed to get detailed information.

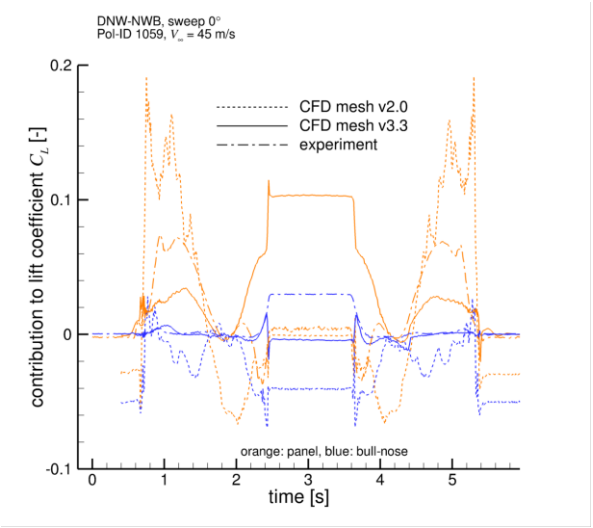

Figure 6: CL comparison between CFD and experimental results

4.2 ONERA meshing strategy

ONERA adopts a more structured approach to meshing. A standard structured mesh is chosen around single components. These individual structured meshes are in turn embedded in a Cartesian background grid.

Specific areas of the Krueger kinematics are considered critical and are further refined by introducing finer meshes. These include the intentional small gap between the Krueger panel

and the bull nose and collar grids when the Krueger panel is fully deployed. Such refinement is necessary as it directly affects the CFD results.

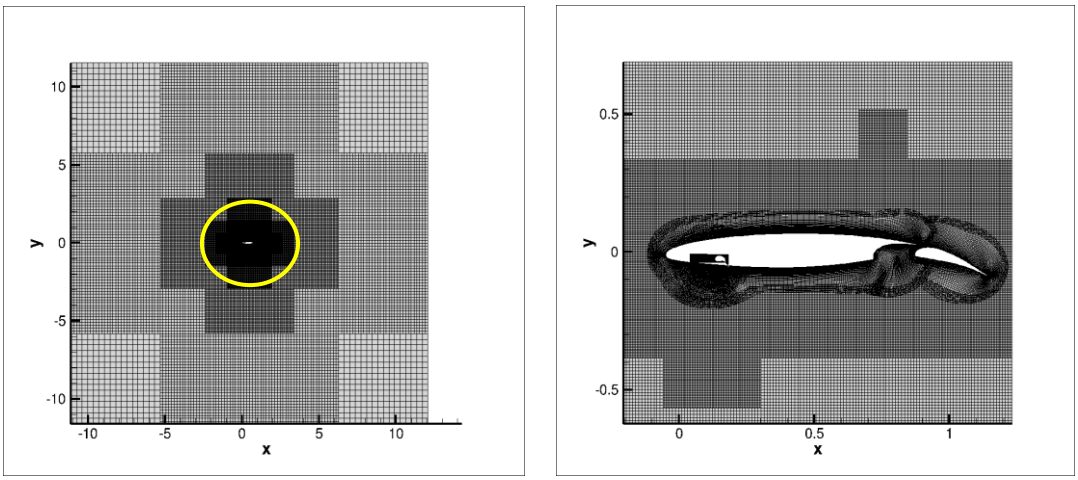

Figure 7: ONERA meshing strategy

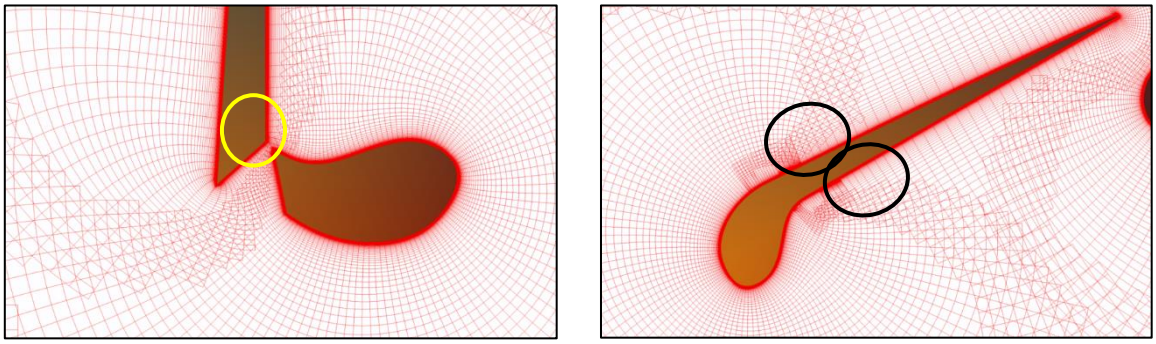

Refined gap between the bullenose and the Krueger panel

Refined gap between the bullenose and the Krueger panel

Figure 8: mesh refinements

4.3 NLR meshing strategy

NLR also adopted structured meshes for individual components, which are in-turn embedded into a structured global mesh. The figure on the left shows the dominant cells of the mesh, and the subordinate overlapping cells are highlighted on the right.

As a demonstration of the Chimera method, the DLR-F15-LLE multi-element airfoil with fully deflected Krüger device is considered. The dominant field cells are shown in Figure 6c, as determined by the Chimera method using the smallest wall distance as main criterion. The other, subordinate cell types are depicted in Figure 6d, showing one layer of buffer cells and two layers of fringe cells that encircle the dominant field cells.

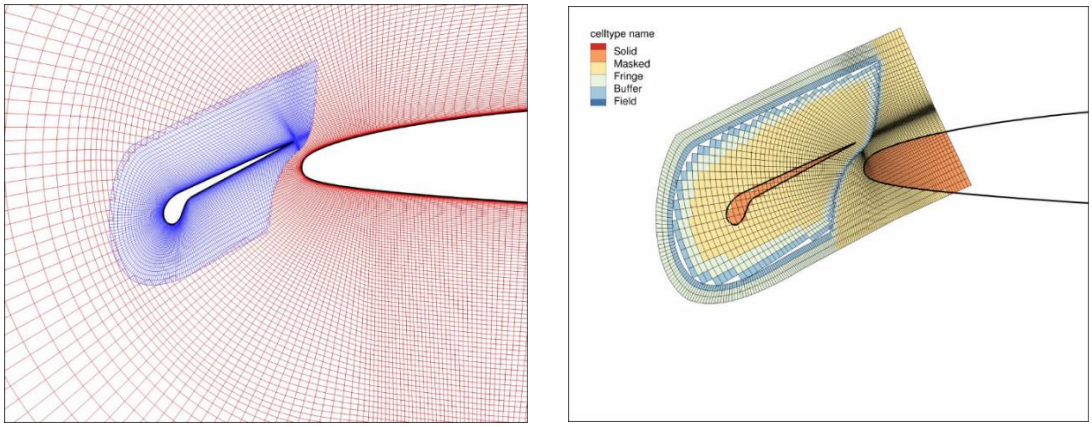

Dominant Cells Subordinate Cells

Figure 9: NLR meshing strategy

4.4 VZLU meshing strategy

VZLU implements cascade meshes, with a combination of structured and unstructured meshes. The individual components, Krueger panel and bullnose, are meshed with structured quad grids. Whereas, the global grid consists of hybrid grid with refined structured grid to capture the wake of the Krueger, as represented in the image below. The hole-cutting algorithm in this case for chimera method implementation is in this case based on wall distance, augmented for multiple parts. The overlapped region needs to be detached from the solid walls, so a small gap is required between the parts. The most challenging regions are: Krueger flap in extended position (small gap between the Krueger panel and the Bull nose), folding of Bull nose (small gap between the Krueger panel and the Bull nose edge) and the fully retracted position (a gap between Krueger panel and the wing cavity). As the data communication occurs only between adjacent grid levels (main wing with Krueger panel, Krueger panel with the Bull nose), slightly higher overlaps may be required to achieve desired results.

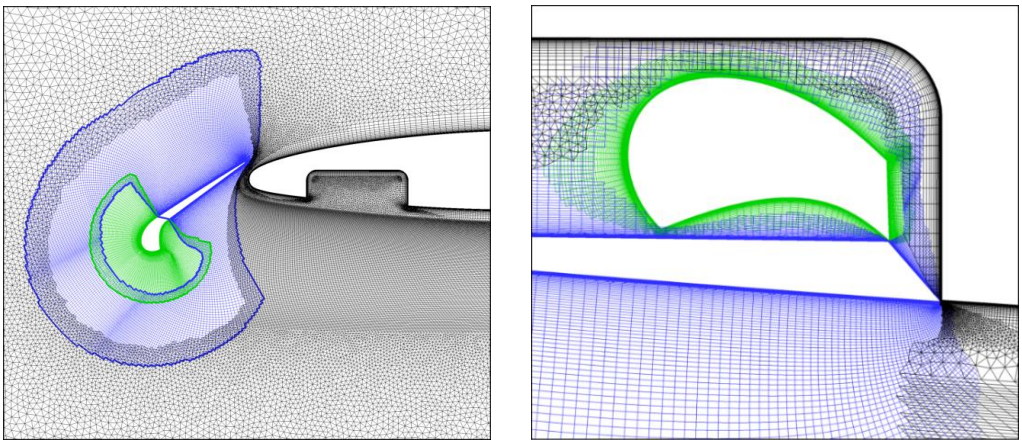

Figure 10: VZLU meshing strategy

5. CFD SIMULATIONS

The meshes generated through various approaches were then subjected to CFD simulations using individual CFD tools. The results were used to carry out a number of observations and comparisons with the experimental results from the three wind-tunnels by each partner. Some of the results are shared below. The work is still undergoing.

The image on the left represents the DNW-NWB model in part-span configuration with a wing sweep of 23 degrees. This particular simulation was performed at 45m/s wind speed with a 1 second hold and 2 seconds Krueger deflection time. Whereas, the image on the right showcases the straight wing in ONERA-L1 wind tunnel in full span configuration. This simulation was performed at a wind speed of 30m/s with 1 second hold and 1 second deflection time. In the CL graph in the top-right corner, the variation of lift-coefficient can be observed along with the Krueger panel deflection. The bottom-right graph shows the pressure distribution at various stages for individual components.

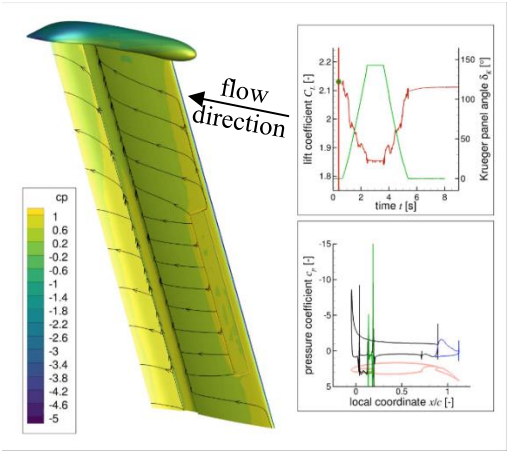

DNW_NWB_partspan_1s2s_u45_23sweep
_view_low_drive_cp

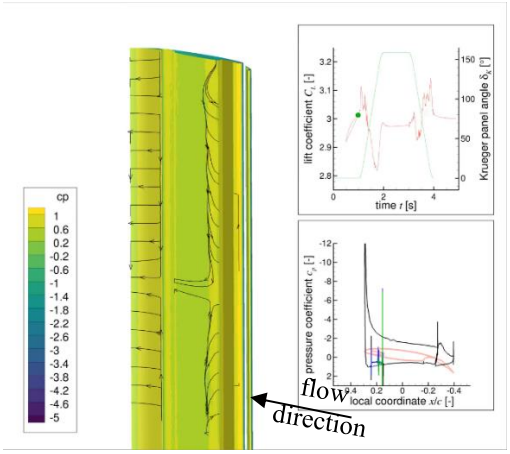

ONERA-L1_fullspan_1s1s_u30_view_
low_drive_cp

Figure 11: Example of the results of CFD simulations

As mentioned, the simulations were performed at various extension and retraction speeds, e.g. 1-4 seconds for the ONERA experiment. The following graphs show pressure distribution for 1 second cycle throughout the movement path during dynamic motion. The solid line represents the Cp distribution during retraction, and the dashed one - extension. It is interesting to note that the two movements follow different paths during motion. The passage of the Krueger flap induces loss of lift. There is a delay between the Krueger panel movement and the reaction of the Cp values on the main wing (red colour).

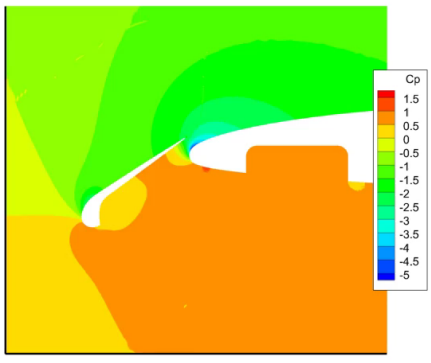

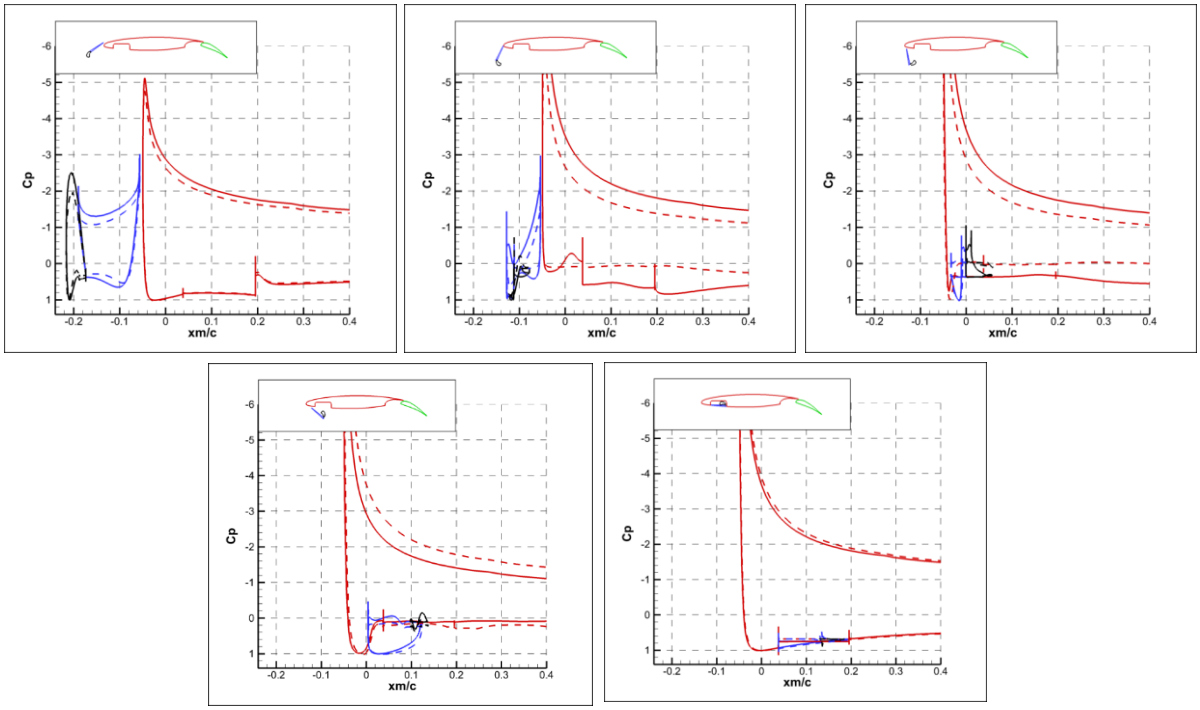

Figure 12: pressure distribution for 1 second condition throughout the movement path during dynamic motion

6. VALIDATION OF CFD RESULTS

6.1 Validation results of DNW-NWB model

Here we consider a two-component Krueger device for static deployment cases, i.e. retracted, full deflected and partially deployed.

The simulations in static cases consider the model in a free air environment where the experimental pressure distribution of the retracted configuration is adopted as a datum solution. The matching incidence angle reads α=9 (degrees) for the wind tunnel condition α=8 (degrees) at an onset velocity V=48.9 m/s.

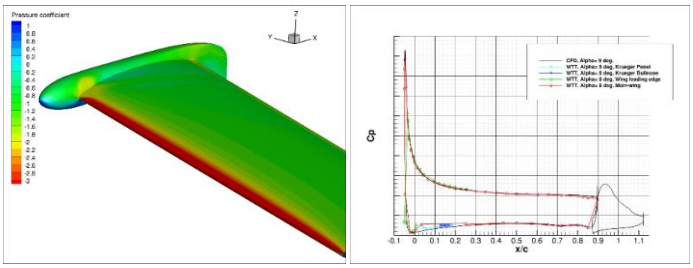

From a flow physics point of view, the cross comparison of the results for the full deflected and retracted configuration reveal the reduction of the suction level at the leading-edge of the main-wing due to the presence of the Krueger device in front of the wing.

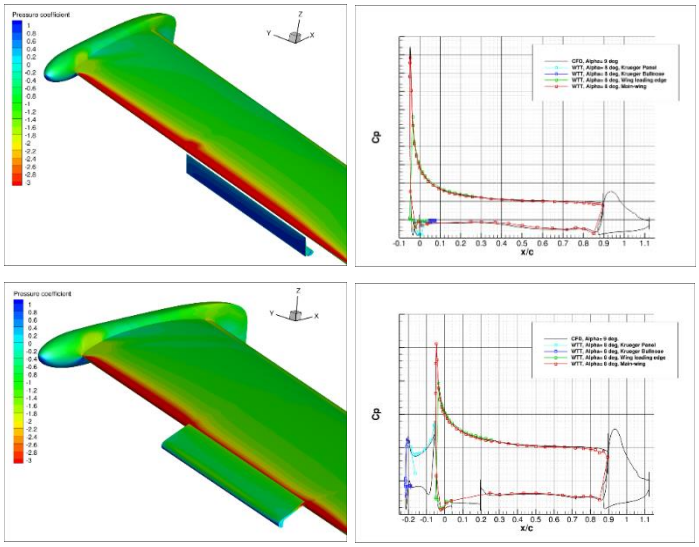

Figure 13: Validation of DNW-NWB model

Furthermore, the cross comparison of the results for the partial deflected and retracted configurations depict the reduction of stagnation pressure at the lower-surface of the main-wing due to a separation region downstream of the Krueger device.

The good agreement of the agreement of the numerical and experimental surface pressure distributions indicate a proper capturing of the flow physics and prediction of the static loads on the various components of the configuration.

In the Cp graphs below, the experimental results are shown with green dots and experimental with dotted and straight lines. The dotted line represents the results from version 2.0 of the mesh, and the thick line represents the final mesh. Snapshots at the bottom of each graph show the Krueger deflection pertaining to each graph. As explained before, it was confirmed that the v3.3 mesh captured the Flow physics very well and agrees with the experimental results significantly. Further work is still needed to gather extensive experimental data to carry out better comparisons between CFD and experimental results.

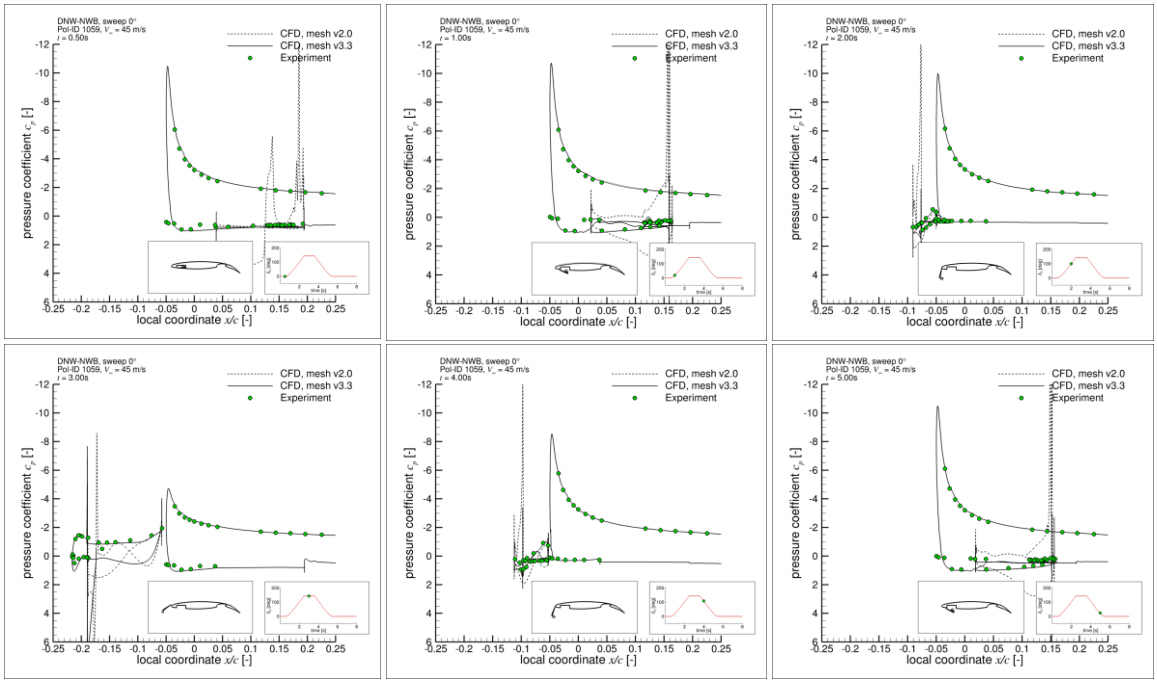

Figure 14: pressure distributions throughout movement path

6.2 Validation results of DNW-LLF model

Here we consider a two-component Krueger device for a dynamic deployment case where the measured time-history of the deployment cycle is adopted which is characterised by a variable rotational velocity. In case of a nominal deployment time of T=2 second, the comparison of the numerical and experimental is presented in the figure below. This concerns the sectional pressure distribution, normal to the leading edge at the centre span station of the part-span Krueger. Time instances for a deflection angle of Θ = 60,80, 100, 120, 140 (degrees) have been selected. The Krueger leading-edge device moves in front of the wing and modifies the leading edge pressure distribution. The selected time instances show that the time-variation to the leading edge pressure distribution is captured (and the time related loss of sectional lift). Furthermore, the sectional pressure distribution on the Krueger elements, i.e. the Krueger panel and the Bullnose, show a good agreement for the experimental and numerical results. This concerns the upper and lower pressure distribution and implies that the time variation of the loads on the Krueger leading-edge device is accurately predicted.

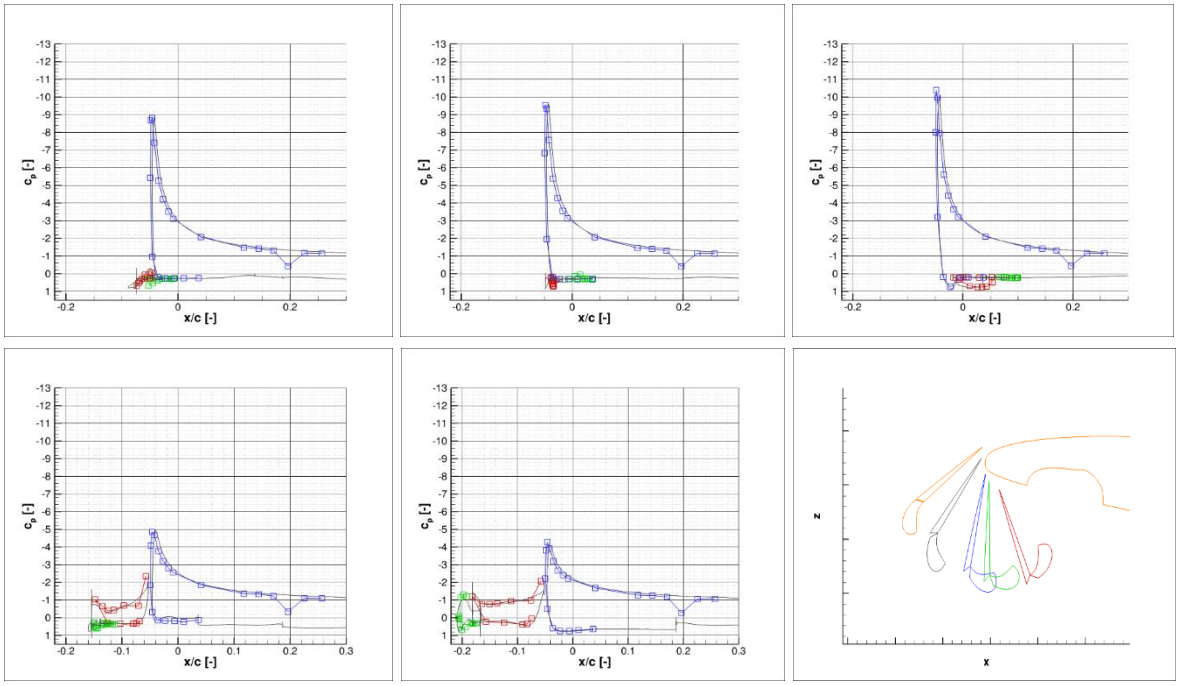

Figure 15: Validation results of DNW-LLF model

7. CHALLENGES FACED DURING WIND-TUNNEL EXPERIMENTS

There were certain obstacles faced during the wind tunnel experiments at all the three wind tunnels. Following image shows the drive and lever speeds during motion. Please note that the drive speed is represented with the colour Blue and the lever speed in orange.

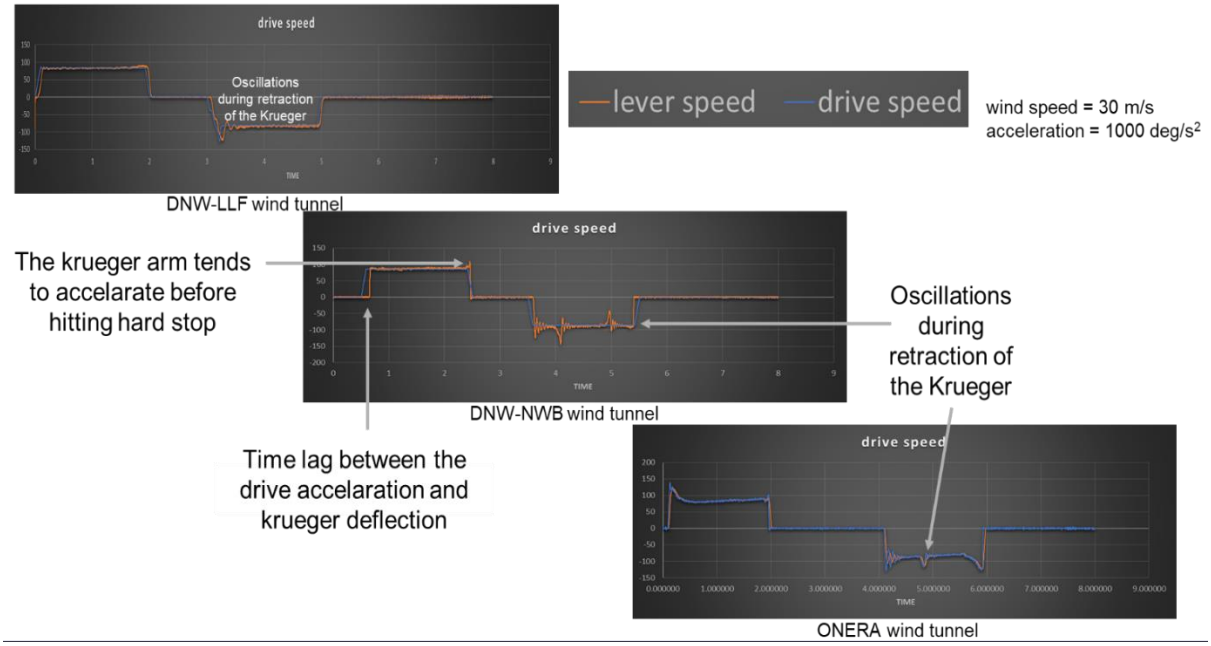

Figure 16: Challenges faced during wind tunnel experiments

It was observed that the Krueger arm tends to accelerate towards the end of extraction. Thus, a mechanical stop had to be introduced to ensure it stopped at the exact desired position.

A time lag was also observed between the drive motion and the Krueger deflection. This is due to the fact that a certain amount of energy is required to set the lever into motion from stationary position.

Furthermore, during retraction, the lever tends to oscillate during retraction. These effects were noted to be less significant in the DNW-LLF tunnel, due to the presence of drive motors on both ends of the wing.

8. CONCLUSION

In this paper, we have described the chimera method for a moving Krueger device along with the lessons learnt during its implementation. The CFD results obtained from this method have been compared with the wind-tunnel experiments carried out at three partner facilities for validation. It can be said that the Chimera prediction method is capable to accurately predict the transient aerodynamic characteristics of a high-lift configuration as well as the changing device loads on the components of a deploying Krueger device. It has been observed that the results are fairly in agreement with the experimental data, but significant efforts are required to overcome the experimental limitations, ensure availability of detailed experimental data and carry out further comparisons between the CFD and wind tunnel results.

ACKNOWLEDGMENT

The project leading to this publication has received funding from the European Union's Horizon 2020 Research and Innovation Framework Programme under the research and innovation programme under grant agreement No 769088.

Furthermore, special thanks are attributed to the entire contributing staff not explicitly named here, mainly all the colleagues contributing to the project – in simulations or experiment, all the colleagues at the testing facilities and all the colleagues running the highly innovative measurement technologies.

REFERENCES

[1] Steger, J. L., Dougherty, F. C. and Benek, J. A., "A Chimera Grid Scheme," Advances in Grid Generation, K. N. Ghia and U. Ghia, eds., ASME FED-Vol. 5, June, 1983.

[2] Meakin, R.L. Moving body overset grid methods for complete aircraft tiltrotor simulations. AIAA paper 1993-3350, 1993.

[3] Blanc, F. Roux, F.-X., Jouhaud, J.-C and Boussuge, J.-F., "Numerical Methods for Control Surfaces Aerodynamics with Flexibility Effects." International Forum on Aeroelasticity and Structural Dynamics, 2009

[4] Iuliano, E., Quagliarella, D. and Wild, J. Krueger High-Lift System Design Optimization, The 8th European Congress on Computational Methods in Applied Sciences and Engineering - ECCOMAS Congress 2022 (2022), Paper-ID 2241.